EPR in dysprosium aluminum garnet at far-infrared frequencies

P. Janssen and M. Mahy
Laboratorium voor Lage Temperaturen en Hoge-Velden Fysica, Katholieke Universiteit Leuven, B-3030 Leuven, Belgium

W. P. Wolf
Section of Applied Physics, Yale University, Becton Center, New Haven, Connecticut 06520
(Received 27 July 1987)

Far-infrared transmission measurements have been made on spherical single crystals of dysprosium aluminum garnet ($Dy_3Al_5O_{12}$) and diluted dysprosium aluminum garnet [$(Dy_{0.1}Y_{0.9})_3Al_5O_{12}$], at frequencies between 157 and 1629 GHz in magnetic fields up to 7.3 T. The strongest resonance was consistent with previous results, corresponding to $g_z = 18.02 \pm 0.07$ and a small internal field. A number of weaker resonances could be identified with sites at which one or more nearest neighbors were reversed. The corresponding interaction parameter $K_1 = (0.8 \pm 0.05) k_B$ is consistent with earlier estimates. In addition, a number of unexpected resonances were observed. Several of these could be identified with Dy^{3+} ions on octahedral crystallographic a sites, having $g_\parallel \approx 10.8$ and $g_\perp \approx 2.8$ and axes along $\{111\}$. The intensities were consistent with estimates based on x-ray data, which indicate concentrations of the order of 1% of a sites occupied by Dy^{3+} ions. The presence of such substitutions may explain various small inconsistencies previously noted in detailed analyses of thermodynamic and neutron-scattering data.

I. INTRODUCTION

Dysprosium aluminum garnet (DyAlG) is generally considered to be a rather well understood material. Extensive studies have shown that it is a low-temperature metamagnet with interesting properties, which can be described in some detail in terms of a relatively simple Ising model.[1] Such a model includes the assumption that the crystal structure is free of imperfections and that the chemical composition is stoichiometric. Support for this assumption seemed to be implied by the existence of large (5 cm^3) optical-quality crystals,[2] and the well-defined crystal structure of the garnets.[3] In this paper we report some far-infrared EPR measurements which show evidence that even apparently high-quality DyAlG crystals can have significant crystal imperfections which will complicate detailed quantitative analyses.

There is, in fact, some earlier evidence that different DyAlG crystals are not identical. Measurements of the magnetic ordering temperature have shown a spread of some 2% and x-ray determinations of the lattice parameter have varied by 0.15%.[2] Optical-absorption spectra have shown some unexplained satellite lines[4] and there have also been reports of anomalous scattering of neutrons near field-induced phase transitions.[5,6] All these effects were quite small and, since there was no direct evidence for their origin, they were ignored in detailed thermodynamic analyses. The present work suggests that the only way to eliminate any such problems is to ensure greater control over crystal stoichiometry.

The use of resonance techniques to study these effects is made possible by the availability of suitable high-frequency sources (150–1700 GHz) and the correspondingly strong magnetic fields up to 7 T. At lower frequencies, the relatively strong spin-spin interactions prevent the observation of resonances in a magnetically concentrated material of this kind. One disadvantage of using very high frequencies is the possibility of complex interference effects (magnetic polariton resonances) due to the short wavelength relative to the sample size.[7] We have observed such effects, especially at the highest frequencies, but we can identify the true magnetic resonances by making measurements at a number of different frequencies and looking for lines which vary linearly with frequency.

The resonances observed in this study were all transitions between the levels of the ground-state Kramers doublet of the Dy^{3+} ions, split by the applied field plus internal fields due to neighboring spins. The long-range contribution to the internal field is usually described as a demagnetizing field and, to ensure that this has a uniform value throughout the sample, it is necessary to use an ellipsoidal sample shape. In an earlier study[8] we have used a relatively thick, irregularly shaped plate which gave a linewidth of 0.85 T (full width at half height). In the present experiments we used a sphere which reduced the linewidth to 0.25 T, but even then we were still not able to resolve any hyperfine structure, which would be expected to extend over about 0.02 T for each of the electronic transitions.[1]

All of the present measurements were made at temperatures below 4.8 K, where none of the higher energy levels are populated. (The lowest one is at 70 cm^{-1}.[9]) Even so, these levels would be expected to have a small but significant effect on the resonances observed. In the presence of a strong magnetic field there will be mixing between the different levels, resulting in small nonlinear contributions to the Zeeman effect. At microwave frequencies these are generally negligible, but in the high fields used at far-infrared frequencies they may become

important. In the present case the mixing effect is enhanced by the relatively large g values of both the ground state ($g=18.1$) and the first excited state ($g_z=-11.1$), and at the highest fields it contributed about 0.5% to the energy-level splitting. Since the effect varies rapidly with field ($\propto B^3$), its influence on the fitted g values and especially the fitted zero-field intercepts can be quite significant. Details of the perturbation calculation are given in the Appendix and the effect on the fitting is discussed in Sec. IV A.

Another unusual feature of DyAlG is the highly anisotropic nature of the ground state. EPR measurements on Dy^{3+} in YAlG have given $g_z=18.3$, $g_x=0.4$, $g_y=0.7$ and these values have been shown to be approximately the same in concentrated DyAlG.[10] One result of this anisotropy is the fact that EPR transitions will be unusually weak and thus more difficult to observe. Correspondingly, it will make other resonances with more isotropic g values *relatively* much stronger, so that observed intensities must be interpreted quite carefully.

Another result of the extreme anisotropy is an enhanced sensitivity to misalignment. This was particularly troublesome in the present experiments, since we had no way to adjust the alignment once the sample was mounted in the magnet. Fortunately, for one orientation, $B\parallel$ [001], the resonance field is at a minimum and the error due to misalignment was negligible,

The experimental arrangement is described briefly in the following section and the results are presented in Sec. III. The discussion in Sec. IV deals with two different classes of resonances: those which can be described in terms of the well-established model of DyAlG and those which cannot. It is the latter which are of particular interest and the implication of this finding is discussed in Sec. V.

II. EXPERIMENT

The experimental arrangement is described in detail elsewhere.[11] We used radiation from a far-infrared laser, optically pumped by a grating-tuned CO_2 laser. The sample was placed in the center of a superconducting magnet with a maximum field of 7.3 T. We measured the radiation transmitted through the sample, using a carbon bolometer. It is important to note that this arrangement detects changes not only of the absorption but also the reflection from the sample.

Table I gives a list of the laser lines used in this work. The laser frequencies were taken from the tabulation by Knight.[12] The magnetic field was calibrated using EPR in the free radical diphenyl picryl hydrazyl (DPPH). Errors in measuring both the field and the frequency were generally negligible compared to the observed linewidths. Temperature could be controlled between 1.5 and 20 K, but most of the experiments were made at the lowest temperatures, where the resolution was best.

Two samples were used in this study. Both were grown by the Linde Division of Union Carbide using the Czochralski method. Sample 1, which we shall designate as "pure" DyAlG, was cut from one of the large samples previously used for the extensive thermodynamic studies reported in Ref. 2. It was carefully shaped and polished to a sphere 6.538±0.003 mm in diameter. Visual inspection showed no evidence of any imperfections or irregularities. Earlier chemical analyses[2] had set rather low limits on possible magnetic impurities (<100 ppm) and the only significant nonmagnetic impurity was only present in less than 1000 ppm. Less well defined was the stoichiometry of the material. The possibility of a deviation from the nominal garnet composition $Dy_3Al_5O_2$ was mentioned in Ref. 2, but no quantitative estimates were made. We shall discuss this problem further in Sec. V.

TABLE I. Far-infrared laser wavelengths after Ref. 12.

Wavelength (μm)	Photon energy (cm^{-1})	Laser gas	Pump line
184	54.4	CD_3OD	10R24
232.94	42.93	CH_3OH	9R10
255	39.2	CD_3OD	10R36
299	33.4	CD_3OD	10R24
305.73	32.709	CH_3OD	9R08
311.55	32.098	HCOOH	10R22
375.54	26.628	CH_2CF_2	10P12
393.63	25.405	HCOOH	9R18
432.6	23.17	HCOOH	9R20
469.02	21.321	CH_3OH	10R38
513.01	19.493	HCOOH	9R28
554.37	18.038	CH_2CF_2	10P14
570.57	17.526	CH_3OH	9P16
699.42	14.298	CH_3OH	9P34
742.57	13.467	HCOOH	9R40
890	11.2	CH_2CF_2	10P22
943.97	10.593	CH_3Cl	9R12
1020	9.804	CH_2CF_2	10P14
1394.06	7.173	C_2H_3Br	10R20
1614.89	6.192	C_2H_3Br	10P26
1899.9	5.263	C_2H_3Br	10P20

Sample 2, which we shall designate as "dilute" DyAlG, had a nominal composition $(Dy_{0.1}Y_{0.9})_3Al_5O_{12}$. It was also shaped and polished to a sphere, 7.62±0.03 mm diameter. Only a few measurements were made on this sample and, since no anomalous lines were observed, no chemical analysis was carried out.

Both crystals were oriented by Laue back reflection. This could be done quite accurately, but mounting the highly polished spheres in the cryostat presented a special problem. We first tried a variety of glues to fix the spheres to the brass ring which fitted the end of the light pipe,[11] but, on cooling (even slowly), these bonds always broke. A satisfactory solution was eventually found by attaching the spheres to a hollow Tufnol (phenolic) plug using Araldite (epoxy) resin and enclosing the assembly with a thin-walled Tufnol tube. This arrangement ensured a reproducible alignment for measurements at different frequencies, but the absolute accuracy of the alignment relative to the field was probably no better than ±3°. The effect of this uncertainty will be discussed for each set of results.

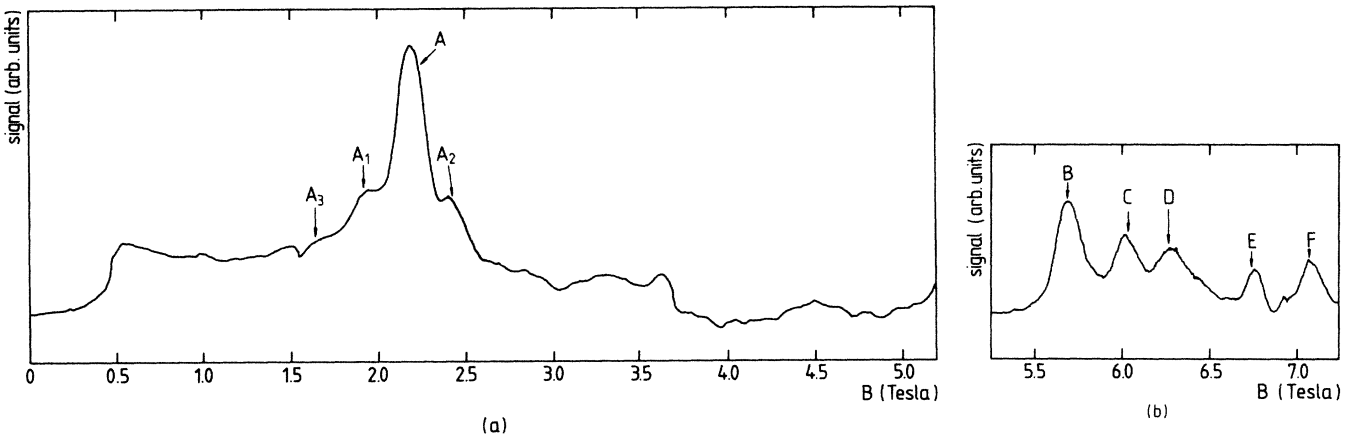

FIG. 1. Absorption vs magnetic field for pure DyAlG with $E=19.493$ cm^{-1}, $T=1.60$ K, and $B\|[001]$. (a) $B=0-5$ T; (b) $B=5.3-7.3$ T.

III. RESULTS

For the "pure" sample, we have results for two orientations, $B\|[001]$ and $B\|[111]$, while for the "dilute" sample measurements were made only with the magnetic field in the [001] direction. Spectra were recorded for a number of fixed laser frequencies by sweeping the field slowly (30 min) from zero to the maximum and measuring the bolometer output.

A. "Pure" sample: $B\|[001]$

Typical spectra at three different laser frequencies and two different temperatures are shown in Figs. 1–3. It can be seen that there are quite a large number of resonances, in marked contrast to the single resonance with $g=g_z$ which might have been expected for this orientation. The linewidths show a marked variation with temperature and frequency, narrowing at low temperatures and high frequencies. Figure 4 shows the peak positions as a function of the laser-photon energy. It is clear that a number of the peaks fall on straight lines, while some of the resonances appear only at specific frequencies. Here we shall concentrate on the resonances which vary approximately linearly with frequency. Fitting the points with an expression of the form

$$E=g\mu_B B+E_0\ , \tag{1}$$

where E and E_0 are measured in cm^{-1} and B in tesla, we obtain the parameters shown in Table II. The intercepts can equivalently be expressed in terms of internal fields $B_i=-E_0/g\mu_B$, which are also shown in Table II.

Several features are immediately apparent.

First, the main line (A) has g value close to the g_z values determined from previous experiments[10] and the small internal field also agrees with earlier estimates.[1] We shall defer more detailed comparisons until we have discussed the effect of the correction due to the third-order Zeeman effect in Sec. IV A.

Second, there are at least three satellite lines (A_1-A_3) with very similar g values, with internal fields which differ from that of the main line by approximately $\pm 2B_1$ and $-4B_1$ where $2B_1\approx 0.3$ T. We shall interpret these

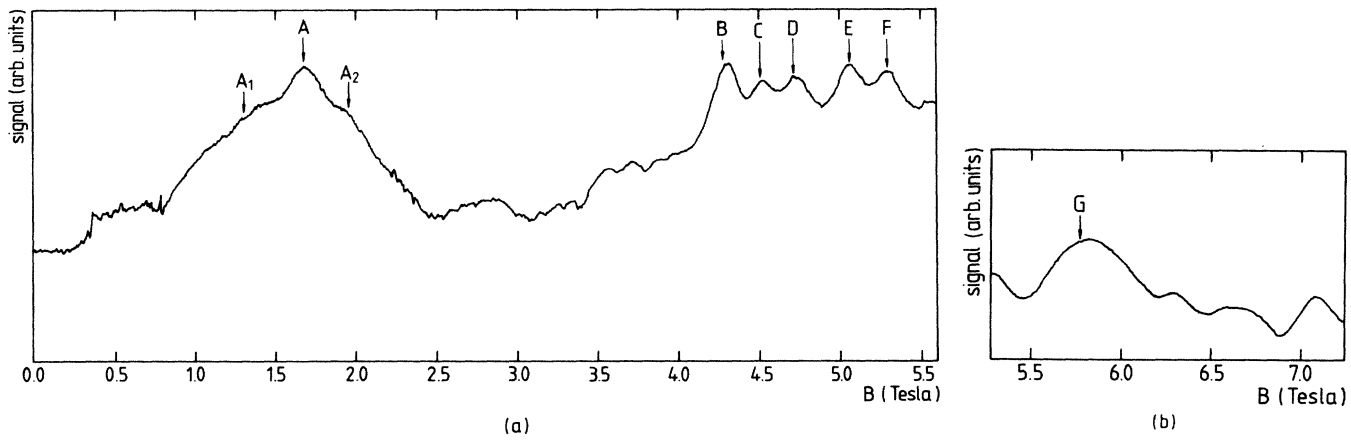

FIG. 2. Absorption vs magnetic field for pure DyAlG with $E=14.298$ cm^{-1}, $T=2.05$ K, and $B\|[001]$. (a) $B=0-5$ T; (b) $B=5.3-7.3$ T.

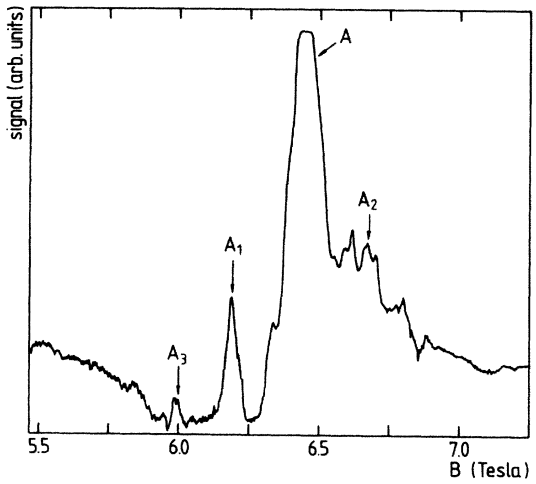

FIG. 3. Absorption vs magnetic field for pure DyAlG with $E=54.4\ \mathrm{cm}^{-1}$, $T=1.63$ K, and $B\|[001]$.

splittings as due to nearest-neighbor spins which are thermally disordered.

Third, there are at least six other lines ($B-G$) with rather similar, but significantly lower, g values which have no immediate explanation in terms of previous analyses of DyAlG. We shall interpret these resonances in terms Dy^{3+} spins on different crystallographic sites.

Fourth, there are a number of other, clearly resolved resonances which appear only at one frequency. We shall offer no detailed explanation for these lines, but it would seem likely that some, if not all of them, are due to interference effects.

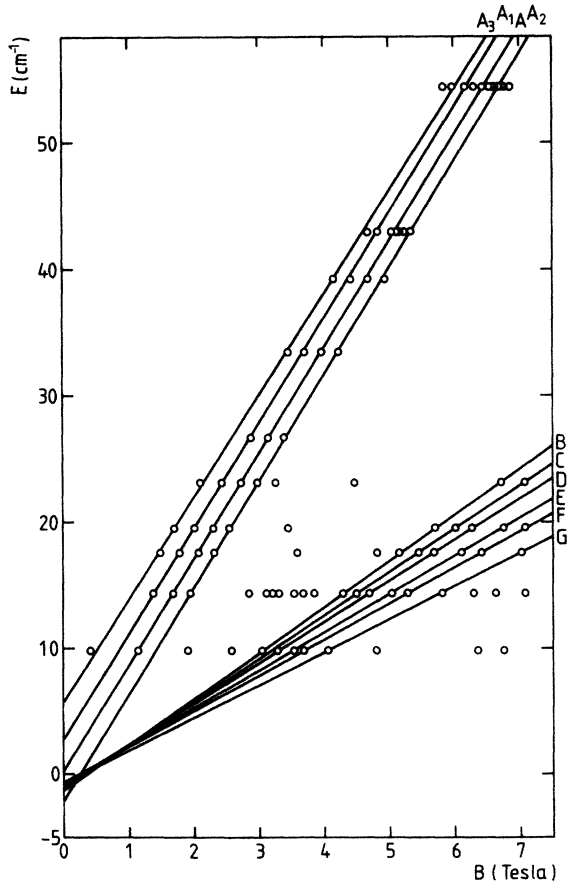

FIG. 4. Peak absorption fields as a function of laser-photon energy for pure DyAlG with $B\|[001]$.

TABLE II. Parameters for pure DyAlG:$B\|[001]$, fitted to Eq. (1).

Line	g	E_0 (cm^{-1})	$B_i=-E_0/g\mu_B$(T)
A_3	17.27±0.18	5.74±0.32	−0.71±0.05
A_1	17.81±0.07	2.77±0.12	−0.33±0.02
A	17.95±0.04	0.23±0.07	−0.03±0.01
A_2	18.11±0.09	−2.20±0.17	0.26±0.02
B	7.76±0.02	−0.18±0.01	0.33±0.01
C	7.33±0.03	−1.11±0.09	0.32±0.03
D	6.94±0.05	−0.86±0.11	0.27±0.04
E	6.44±0.02	−0.82±0.06	0.27±0.02
F	6.09±0.04	−0.71±0.12	0.25±0.04
G	5.57±0.04	−0.77±0.12	0.30±0.05

We may also note the unusual line shape at the highest frequency (Fig. 3). The flat top corresponds to zero detector signal, i.e., zero radiation transmitted by the sample. To check that this effect was not due to power saturation, we decreased the laser power until the signal was barely visible above the detector noise, but no change in line shape was observed. We conclude that the high absorption is simply due to the relatively large sample thickness compared to the wavelength. This effect will be most marked at the highest frequencies, as observed.

No attempt was made to study the line shapes or, indeed, the linewidths. We observed qualitatively that the lines become narrower at the highest field and at the lowest temperatures. Typical linewidths were then 0.25 T. As the temperature was raised, the lines broadened quite rapidly, and by 4 K there are only one unresolved line of the order 1 T wide.

B. Dilute sample: $B\|[001]$

A typical spectrum is shown in Fig. 5. The most striking feature is the fact that the low-g-value resonances ap-

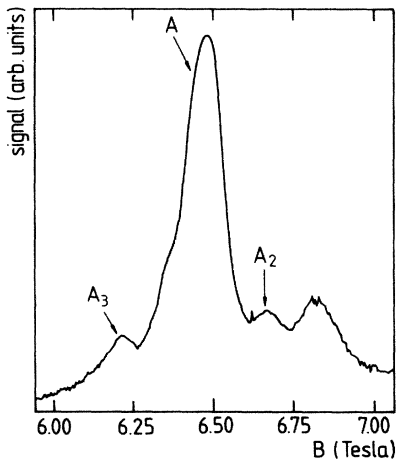

FIG. 5. Absorption vs magnetic field for dilute DyAlG, $(Dy_{0.1}Y_{0.9})_3Al_5O_{12}$, with $E=54.4\ \mathrm{cm}^{-1}$, $T=1.60$ K, and $B\|[001]$.

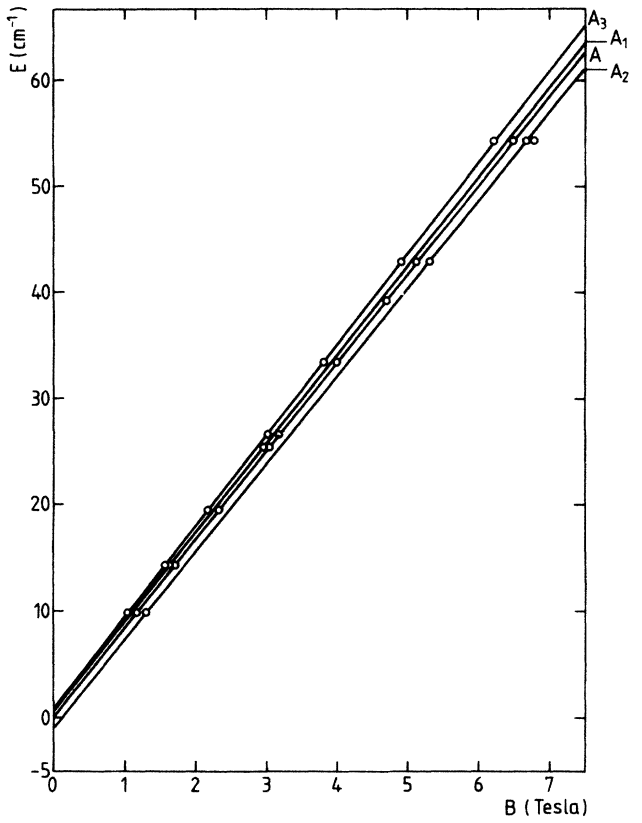

FIG. 6. Peak absorption fields as a function of laser-photon energy for dilute DyAlG with $B\|[001]$.

parent with "pure" samples have disappeared even though the signal-to-noise ratio was comparable to the experiments on the concentrated sample. Only the main resonance (A) and three satellites (A_1-A_3) with nearly the same g value were detected. The results are summarized in Fig. 6 and the parameters from a fit of the form of Eq. (1) are given in Table III.

The lines observed for this sample were somewhat narrower ($\sim$0.15 T) than for the "pure" sample, but again no detailed study of the linewidth was made.

C. "Pure" sample: $B\|[111]$

Typical spectra for three different laser frequencies are shown in Figs. 7–9. These spectra were all taken at the same, relatively high temperature of 4.8 K. A marked narrowing with increasing frequency is again apparent. The location of the resonance peaks is summarized in Fig. 10 and the corresponding fitting parameters are

TABLE III. Parameters for dilute DyAlG:$B\|[001]$, fitted to Eq. (1).

Line	g	E_0 (cm^{-1})	$B_i=-E_0/g\mu_B$(T)
A_3	18.38±0.04	0.84±0.06	−0.10 ±0.01
A_1	17.92[a]	0.60[a]	−0.072[a]
A	17.90±0.04	0.03±0.06	−0.004±0.01
A_2	17.74±0.08	−1.00±0.19	0.12 ±0.02

[a]Based on two data points.

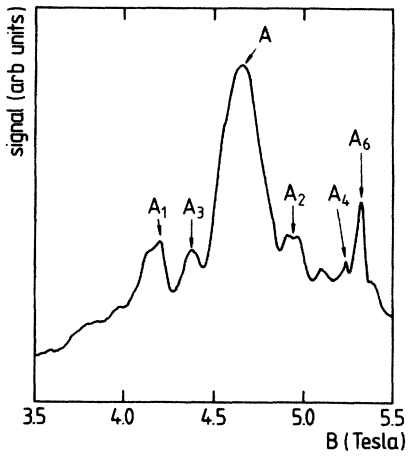

FIG. 7. Absorption vs magnetic field for pure DyAlG with $E=23.17$ cm^{-1}, $T=4.8$ K, and $B\|[111]$.

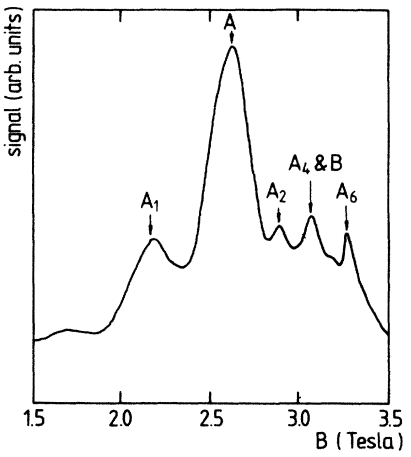

FIG. 8. Absorption vs magnetic field for pure DyAlG with $E=13.467$ cm^{-1}, $T=4.8$ K, and $B\|[111]$.

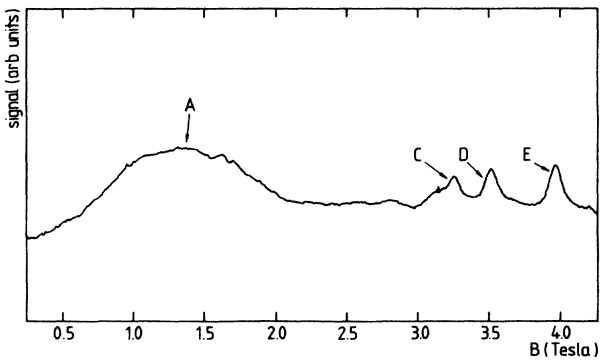

FIG. 9. Absorption vs magnetic field for pure DyAlG with $E=5.263$ cm^{-1}, $T=4.8$ K, and $B\|[111]$. The structure around the peak A becomes more clearly resolved at lower temperatures.

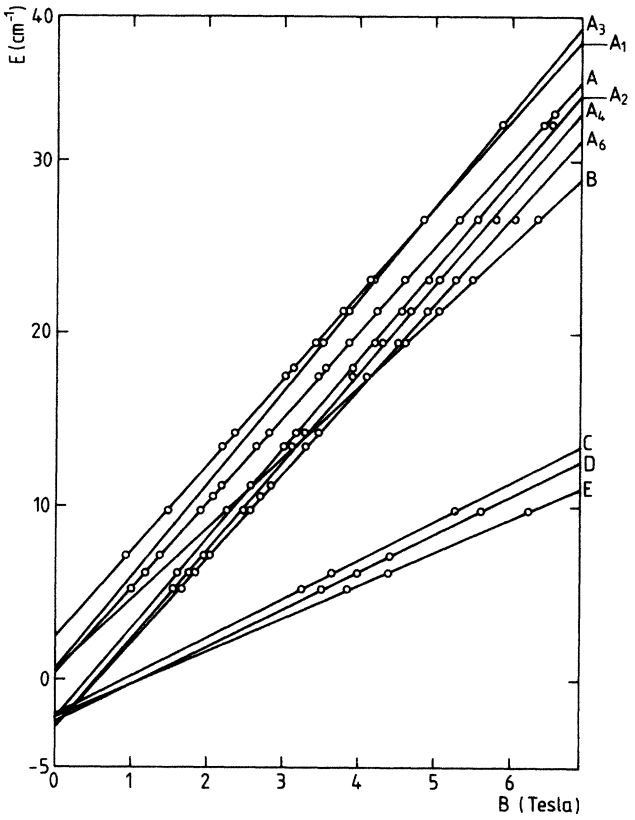

FIG. 10. Peak absorption fields as a function of laser-photon energy for pure DyAlG with $B\|[111]$.

given in Table IV. Here, again, we find a number of satellites (A_1-A_6) to the main resonance (A) with nearly the same g value. Also, a number of low-g-value lines (C, D, and E) were observed, together with one resonance (B) having an intermediate g value. Linewidths are generally similar to those for $B\|[001]$; the width of the main line A was of the order of 0.25 T.

The most striking feature of those results is the appearance of the large number of resonances. On the basis of previous work, one would expect one or, at most, two closely resolved lines, but the observed spectrum is quite unexpected. At higher temperatures the lines broadened quite rapidly and quickly became unresolved. This variation was not studied in detail, and the results which were used for the final analysis were all obtained at the lowest attainable temperatures, 1.6–1.7 K.

TABLE IV. Parameters for pure DyAlG:$B\|[111]$, fitted to Eq. (1).

Line	g	E_0 (cm^{-1})	$B_i=-E_0/g\mu_B$(T)
A_6	10.47±0.04	−2.95±0.06	0.60±0.01
A_4	10.51±0.04	−2.53±0.06	0.52±0.01
A_2	10.66±0.18	−1.82±0.25	0.37±0.05
A	10.47±0.03	0.32±0.04	−0.07±0.01
A_1	10.49±0.05	2.52±0.06	−0.51±0.01
A_3	11.08[a]	0.55[a]	−0.11[a]
B	8.72[a]	−0.05[a]	−0.12[a]
C	4.74±0.02	−1.98±0.04	0.90±0.02
D	4.61±0.06	−2.44±0.12	1.13±0.06
E	4.05±0.11	−2.16±0.22	1.14±0.12

[a]Based on two data points.

IV. DISCUSSION

A. "Pure" sample: $B\|[001]$

1. Main resonance

Two resonances are to be expected: one with $g=g_z\approx 18$ and one having $g=[(g_x^2+g_y^2)/2]^{1/2}\approx 0.5$.[10] The latter was far outside our available field and/or frequency region and was not observed. Therefore, the main line A should have $g=g_z$. The fitted value in Table II is clearly in reasonable agreement with our expectations. Before we can make a detailed comparison with previous g-value determinations, however, we must consider the effect of third-order Zeeman effect corrections which, as mentioned previously, may not be negligible in high-field experiments such as these.

Details of the correction are discussed in the Appendix. The final result for the energy splitting is

$$E=g_z\mu_B B[1-(0.8\pm 0.3)\times 10^{-4}B^2]\,, \tag{2}$$

where B is measured in tesla. At the highest fields the correction is thus less than 0.5%, but it is not entirely negligible. Even though the curvature in the E versus B plots implied by Eq. (2) cannot be detected with the present experimental accuracy, the presence of a small term in B^2 will affect the fitted parameters. To allow for this effect we divide E by the correction factor at each field and refit

$$E'=E/[1-(0.8\pm 0.3)\times 10^{-4}B^2]$$

for lines A, A_1-A_3 as a function of B. The results are shown in Table V.

It can be seen that the effect on the g values is quite small, as one would expect, but the zero-field intercepts B_1 are affected by proportionality larger amounts. This simply reflects the difficulty of inferring small shifts from high-field extrapolations. We will discuss an alternative fitting procedure in the next section.

The g value of the main line, $g_z=18.02\pm 0.07$, can now be compared with previous experimental determinations. A good summary of these is given in Ref. 1 and, taking a weighted mean, we find 18.18±0.12 in good agreement with our value.

The corresponding internal field $B_i=-0.02\pm 0.02$ T

TABLE V. Parameters for pure DyAlG:$B\|[001]$, corrected using Eq. (2).

Line	g	E_0 (cm^{-1})	$B_i=-E_0/g\mu_B$(T)
A_3	17.34±0.18	5.70±0.32	−0.70±0.05
A_1	17.88±0.07	2.70±0.12	−0.32±0.02
A	18.02±0.04	0.17±0.07	−0.02±0.01
A_2	18.19±0.09	−2.29±0.17	0.27±0.02

may be compared with the results of previous estimates of the Curie-Weiss temperature θ_1. B_i is proportional to θ_1 (Ref. 1):

$$\theta_1 = g_z \mu_B B_i / 2k_B \ . \tag{3}$$

Thus, our value of B_i corresponds to $\theta_1 = -0.12 \pm 0.12$ K. This may be compared to previous estimates ranging from 0.20 ± 0.15 K to -0.13 ± 0.3 K.[10] It is clear that θ_1 is very small and difficult to determine accurately. The reason for the smallness of θ_1 is discussed elsewhere.[1,13] It arises from an unusual cancellation of near-neighbor interactions resulting from the garnet structure and the large anisotropy in g.

No detailed study was made of the linewidth, but we may note a number of qualitative features. First, there is clearly a significant contribution which increases rapidly with temperature. This is, presumably, due to spin-lattice relaxation effects. At the lowest temperatures this contribution should be quite small. Second, we would expect quite a large contribution from spin-spin interactions since two-thirds of the spins are not ordered in the presence of a magnetic field parallel to [001]. (This is not true at temperatures below about 1 K, where the spins perpendicular to $B \| [001]$ order antiferromagnetically,[14] but at the temperatures of the present measurements they should be largely disordered.) The disorder in these transverse spins will result in a distribution of internal fields at the sites at which resonance is observed. We will discuss this effect further in the next section in connection with some of the unresolved satellite lines which were observed.

2. *Satellites*

The lines which appeared at different frequencies with essentially the same g value as the main line can be interpreted in terms of interactions with near neighbors. If we consider a particular spin in resonance with a field parallel to the z axis, we note that it has four nearest neighbors whose large-g-value axes are along x and y, perpendicular to the field. To a first approximation, these spins will not be affected by the field and they will be disordered, with equal probabilities of pointing along $\pm x$ and $\pm y$, respectively. If we denote by B_1 the contribution to the internal field which any one of these neighbors will make at the site in resonance, the four neighbors together will produce fields of $4B_1$, $+2B_1$, 0, $-2B_1$, and $-4B_1$, with relative probabilities of 1:4:6:4:1.

The field B_1 can be calculated from the interaction parameters given by Schneider *et al.*:[15] $K_1 = K_1^{\rm dip}(1+\alpha_1) = (0.770 \pm 0.052)\ k_B$, where K_1 describes the Ising-like spin-spin interaction and α_1 allows for the nondipolar interactions. This value corresponds to an internal field

$$B_1 = 2K_1 / g_z \mu_B = (0.126 \pm 0.009)\ \text{T} \ , \tag{4}$$

and this can be compared to the measured line shifts. In principle, these can be obtained from the fitted straight lines in Fig. 4 and Table V, but we note that the fits give slightly different g values and that small changes in g_z greatly affect the internal field intercepts. We, therefore, refitted the data using the same g value for the satellites as for the main line. The results are shown in Table VI.

It can be seen that the splittings, respectively divided by two and four, agree quite well with one another and with the value of B_1 estimated from K_1. The mean value $B_1 = (0.132 \pm 0.008)$ T is slightly higher than our previous estimate [Eq. (4)], but it is well within the experimental uncertainties. We can conclude, therefore, that the satellites $A_1 - A_3$ are due to interactions with the four nearest neighbors.

There are several factors which complicate this simple picture. First, it is evident from Figs. 1–3 that the relative intensities are not in the ratio 1:4:6:4:1, as predicted. There can be at least three reasons for this.

If the magnetic field is slightly misaligned from [001], it will have components along $\pm x$ and $\pm y$ and the neighboring spins will not be completely disordered. This will decrease the intensity of the satellites, with the outer lines decreasing more strongly than the inner lines. In the limiting case in which both x spins are completely aligned in the same direction, their contribution to the internal field will tend to zero,[13] and similarly this happens for the y spins.

The second reason for a change in the relative intensities is short-range order, resulting from the interactions of the x and y spins among themselves. These are the interactions which lead to a new antiferromagnetic state below about 1 K,[14,16] and it is clear that there will be a considerable amount of short-range order at the temperature of our measurements 1.6–1.7 K. In the limit of perfect antiferromagnetic order, the x and y spins would produce internal fields of $\pm 4B_1$, at the sites of the z spins, with corresponding satellite lines. With only partial antiferromagnetic order, internal fields of $\pm 2B_1$ and 0 would also be allowed, corresponding to the reversal of one or two spins from the antiferromagnetically ordered state. Thus short-range order would again lead to the same satellite pattern as complete disorder among the x and y spins, but with a rather different intensity distribution. There is no simple way to calculate the intensities for this situation, but it is not surprising that the observed intensities are not the same as those predicted on the basis of complete disorder.

The third complication arises from the fact that the interactions are not, of course, limited to nearest neighbors. Each z spin has, in addition, eight next-nearest neighbors, eight fourth-nearest neighbors, etc., which also make significant contributions to the internal field. Since there is a relatively large number of near neighbors and the field contribution from each is quite small, one might not expect to resolve the different configurations, and no such

TABLE VI. Internal-field line shifts for pure DyAlG:$B \| [001]$, corrected using Eq. (2) and fixing $g(A) = 18.02$.

Line	$B_i = -E_0/g\mu_B$(T)	$[B_i - B_i(A)]$(T)
A_3	0.546 ±0.038	0.526±0.046
A_1	0.296 ±0.014	0.276±0.022
A	0.020 ±0.008	
A_2	−0.0238±0.020	−0.258±0.028

structure was indeed observed. However, it is clear that these neighbors can contribute to the linewidths of the resonances which are observed.

We should also note a possible alternative mechanism which might explain some of the satellite lines, but which seems to be relatively unimportant in view of the experimental results. If some of the Dy^{3+} ions were replaced by nonmagnetic Al^{3+} ions, or by vacancies, the above discussion would be modified by the addition of extra satellites at $\pm B_1$, corresponding to the absence of one nearest-neighbors Dy^{3+} ion. Given the approximate value of B_1 known from earlier work [Eq. (4)] and the fact that the principal satellites agree closely with the value $\pm 2B_1$, we can effectively exclude this mechanism in the present situation.

3. Linewidths

If one could specify the state of disorder of the x and y spins, one could make an estimate of their contribution to the linewidth by calculating suitable averages of their internal fields at a z site. For example, we can estimate the root-mean-square field due to the $n(=8)$ second-nearest neighbors from the interaction parameter K_2:

$$\langle (B_2)^2 \rangle^{1/2} = A_n (2K_2/g_z \mu_B) , \tag{5}$$

where A_n is a constant which reflects the disorder of the neighbors. If we assume that they are completely random, so that they set up a field distribution with binomial probabilities, $A_n = \sqrt{n} = \sqrt{8}$. Substituting the value of $K_2 = 0.159\ k_B$ given in Ref. 15, we find for the rms internal field

$$\langle (B_2)^2 \rangle^{1/2} = 0.074 \text{ T} . \tag{6}$$

The rms internal field may be compared approximately with the half-width at half-height of the resonance line. (For a Gaussian line shape the rms field $=0.85$ times the half-width at half-height.) Thus our estimate gives for the full linewidth

$$\Delta B \approx 0.17 \text{ T} . \tag{7}$$

This value is comparable to the magnitudes of the observed linewidths, but it cannot be compared directly because the spins are not really random, as discussed above. Lack of randomness would reduce the rms field. On the other hand, we should really also include contributions from more distant neighbors, and this would increase the rms field. We can only conclude, therefore, that the observed linewidths are not unreasonable and due mainly to spin-spin interactions.

There is, in fact, one additional mechanism which will make a contribution and which we have not considered so far: unresolved hyperfine structure with Dy nuclear spins. This effect is relatively small and we may ignore it here, but we must consider it when we discuss the case of $B \| [111]$, since then the mechanism discussed above should not contribute. We shall return to this in Sec. IV C.

4. Low g-value resonances

The resonances $B-G$ are completely unexpected on the basis of previous experiments on DyAlG. Their explanation must be sought, therefore, in terms of some sort of "impurity."

At first this seems unlikely since they have intensities which are not much less than that of the main line. However, this aspect may be explained by noticing that *all* the lines observed are actually rather weak, so that the extra lines could, in fact, be due to a relatively small concentration of impurity spins, if these had more isotropic g values.

The most obvious source of impurities would be other rare-earth ions, substituting for some of the Dy^{3+} ions. However, all of the rare-earth ions with Kramers ground states have been studied in the garnets[17] and none of their g values correspond to the resonances which we have observed here. Also, there are too many lines to be caused by any one impurity.

We will seek an explanation for these lines in terms of deviations of stoichiometry, but we defer the discussion until we have reviewed the [111] data, which also show extra low-g-value lines.

B. Dilute sample: $B \| [001]$

From the fit of Table III, we see that the main resonance has a g value consistent with that of the pure sample, as one might expect. The internal-field intercept B_i is very small, again as one might expect, since the internal field should scale with concentration. One may note that the third-order Zeeman correction here actually changes the sign of the intercept, emphasizing the difficulty of estimating this small quantity.

A quantitative analysis of the three satellites around the main line is, likewise, difficult in this case. There are two complications. First, we must note that in a diluted sample not all of the four-nearest-neighbor sites will be occupied by Dy ions, so that we can now expect shifts of $\pm B_1$ and $\pm 3B_1$ as well as the four values found previously. However, not all of these will be resolved, since the structural disorder will add to the linewidth and, indeed, no more than three lines were ever observed. At some frequencies no satellites at all were seen.

The second, and even more serious, complication arises from the fact that we must expect small shifts in the g value corresponding to different crystallographic configurations. It is not reasonable, therefore, to repeat our previous procedure of assuming a single g value for all of the satellite lines in fitting the splittings.

Given the uncertainties of extrapolating the fits in general, and especially with relatively few data points, we can only conclude that the internal field intercepts given in Table III are qualitatively consistent with nearest-neighbor spin-spin interactions, but we can draw no further quantitative conclusions.

The most interesting result from the dilute sample is the fact that no low-g-value lines were observed, even though there was ample signal-to-noise ratio had they been as intense as in the "pure" sample. If we assume that the previously observed lines were due to lack of

stoichiometry, we must conclude that either Dy^{3+} has a greater preference for the "proper" crystallographic c sites than does Y^{3+}, or that the dilute sample was simply closer to stoichiometry in the way it was grown.

In any case, this result shows that not all garnet crystals are the same.

C. Pure sample: $B\|[111]$

1. Main line

For this orientation two resonances with very similar g values are to be expected: one with $g_a=[(g_z^2+2g_x^2)/3]^{1/2}$ and one with $g_b=[(g_z^2+2g_y^2)/3]^{1/2}$. Since g_x and g_y are known to be very small,[10] these two resonances will appear as one with $g=g_z/\sqrt{3}$. From the fit in Table IV we find for the main line $g=10.47\pm0.03$, which agrees very well with

$$g=(18.18\pm0.12)/\sqrt{3}=10.50\pm0.07$$

estimated from previous work.[10] Here we have not applied the small correction due to the third-order Zeeman effect because much larger uncertainties from misalignment and the nonzero vales of g_x and g_y in any case preclude a detailed comparison. However, we can conclude that the main line agrees very well with our expectations.

For the same reasons there is also no point in examining the internal field intercept B_i in detail, but we may note that it is once again very small, as we would expect.

The linewidth will have four contributions: a part due to the two unresolved resonances corresponding to $g_a=[(g_z^2+2g_x^2)/3]^{1/2}$ and $g_b=[(g_z^2+2g_y^2)/3]^{1/2}$, a contribution from hyperfine structure, an intrinsic part, and a possible part due to misalignment. The part due to $g_a\approx g_b$ can be calculated from estimates of g_x and g_y. The splitting is approximately

$$\delta B_{xy}=[(g_x^2-g_y^2)/g_z^2]B_{[111]}\ , \tag{8}$$

and taking $g_x\approx0.7$, $g_y\approx0.4$ this gives $\delta B_{xy}\approx0.001\ B_{[111]}$, where $B_{[111]}$ is the resonance field along [111]. At the highest frequencies, δB_{xy} is thus ~0.06 T and it will decrease linearly with frequency.

Over much of the frequency range, this splitting will be comparable with the unresolved hyperfine structure due to the two isotopes ^{161}Dy and ^{163}Dy which each have spin $I=\frac{5}{2}$. The hyperfine splittings can be calculated from the coupling constants A and P determined from Mössbauer experiments, or estimated from other EPR experiments.[10] The overall hyperfine splitting is thus found to be 0.02 T.

In practice, both of these contributions may well be overshadowed by the effect of misalignment. A simple estimate shows that the three lines corresponding to spins with their large g-value axes parallel to [100], [010] and [001] will be split by

$$\delta B_\theta\sim0.025\ B_{[111]}\cdot\theta\ , \tag{9}$$

where θ is the angle of misalignment of the field from [111] measured in degrees. For *small* misalignments, this will result in a further broadening of the main resonance line. For values of $\theta\approx2°$ or more, we would expect three resolved resonances *with approximately equal intensities* and, because no such spectrum was in fact observed, we can conclude that the alignment was indeed quite good. However, we can not rule out a significant contribution to the linewidth.

It is clear that all these effects will mask the intrinsic linewidth, which we might expect to be quite narrow for this orientation, since the spin-spin contributions, important for $B\|[001]$, will here be suppressed by the strong field acting on all spins. It should be interesting to see if correspondingly narrow resonances could be observed for less symmetrical orientations, where all the degenerate lines are resolved.

2. Satellites

The mechanism invoked for the explanation of the satellites around the main line for $B\|[001]$ does not predict any extra lines for $B\|[111]$. This is because all spins now experience large field components along their local g_z axes, so that they will all be almost completely polarized at low temperatures. The probability of a spin reversal will be proportional to $\exp[-(g_z\mu_B B/\sqrt{3}k_B T)]$, which at $T=1.8$ K and $B=5$ T is equal to $e^{-19.6}\approx3\times10^{-9}$. Different combinations of internal fields due to spin reversals are thus very unlikely.

If we examine Fig. 10, we can see that the satellites may be divided into three groups.

(i) Lines A_1 and A_6 have almost the same g values, equal to that of the main line, and almost equal and opposite internal fields.

(ii) Lines A_3 and B have very small internal field intercepts, close to that for the main line. Their average g value ($g=10.15$) is close to that of the main line ($g=10.45$).

(iii) Lines A_2 and A_4 have similar g values and somewhat similar internal fields, but both intercepts are large and positive.

There is no immediately obvious explanation for either group (i) or (iii). For group (i) it seems tempting to postulate some mechanism which simply provides a field of ±0.5 T at some of the normal Dy^{3+} sites, but we have been unable to find any physically reasonable mechanism. One would need some sort of impurity, which would be polarized by the applied field, and which could provide positive and negative internal fields at different sites. Such a mechanism might also explain A_2 and A_4, but here we have only found a positive internal-field intercept.

Lines A_3 and B, on the other hand, do have a simple explanation. If we postulate that some of the crystal a sites, normally occupied by Al^{3+}, may be occupied by Dy^{3+} in low concentration, we would expect a number of extra resonances. These would include, primarily, resonances from c sites which happened to have an a-site Dy^{3+} neighbor, and from the a-site Dy^{3+} spins themselves.

For a c site perturbed by an a-site neighbor, we would expect a g tensor with different axes and generally different principal values. However, since Dy^{3+} has the

same charge as the Al^{3+} which it replaces, and the only effect therefore arises from its larger ionic radius (0.91 Å versus 0.51 Å), we might expect the change in the g tensor to be relatively small and of the form

$$\vec{\vec{g}}=\vec{\vec{g}}_0+\delta\vec{\vec{g}}\ , \tag{10}$$

where $\vec{\vec{g}}_0$ is the unperturbed value which is dominated by one component, g_z, and $\delta\vec{\vec{g}}$ is a tensor with components $\delta g_{\alpha\beta}$, where α, $\beta=x,y,z$ are any arbitrary set of axes. For convenience we will take x,y,z to be the cubic axes. (Note that these are then not the same axes as the usual local D_2 axes, except that the z axes coincide.)

For a field in the [111] direction the Zeeman splitting will then be given by $g_e\mu_B B$, where

$$g_e=[(g_z+\delta g_{zz})+2(\delta g_{zx}+\delta g_{zy})]/\sqrt{3}\ . \tag{11}$$

We thus have a mechanism for finding a shifted g value. To check its reasonableness, we must examine the effect of different neighbor sites being occupied. Each c site has four nearest-neighbor a sites at $(\pm a/4,\ 0,\ a/8)$ and $(0,\ \pm a/4,\ -a/8)$. Thus, if the above expression for g_e applies to one of these sites occupied, the g value for all four cases will be

$$g_e=[(g_z+\delta g_{zz})+2(\pm\delta g_{zx}\pm\delta g_{zy})]/\sqrt{3}\ , \tag{12}$$

We might, therefore, expect four lines, but if either $g_{zx}\gg$ or $\ll g_{zy}$ we would get only two. If $g_{zx}\simeq g_{zy}$ we would get three lines, but one of these would have $g_e\approx 1/\sqrt{3}(g_z+\delta g_{zz})$, which would probably be unresolved from the main line.

If we identify lines A_3 and B with

$$g_e=1/\sqrt{3}[(g_z+\delta g_{zz})\pm 2\delta g]\ , \tag{13}$$

we obtain $\delta g=1.2$, $\delta g_{zz}=-0.5$, where we have written δg for either δg_{zx}, δg_{zy} or $(\delta_{zx}+\delta_{zy})$ depending on which term is dominant. These magnitudes are not unreasonable. If we were to interpret the off-diagonal components in terms of a simple tilt of the local z axis, the angle of tilt would be about 7°.

It is important to check that this explanation is also consistent with the results for $B\|[001]$. Using the value of δg_{zz} estimated above, we predict an extra line split from the main resonance by less than 0.1 T, which is within the linewidth of the observed resonance.

It is not unreasonable to conclude, therefore, that at least two of the observed resonances are due to the effect of Dy^{3+} ions on a sites, but further evidence is needed. Some of this is provided by the analysis of the low-g-value lines.

3. *Low-g-value lines*

The model in which a small number of Dy^{3+} ions occupy a sites also predicts additional resonances from these spins themselves. The point symmetry of the a sites is $\bar{3}$, so that the g tensor will be characterized by two principal values: $g_\parallel$ and $g_\perp$ relative to the threefold axis. There are eight a sites in the unit cell, but only four are magnetically inequivalent; they are characterized by their threefold axes along [111], $[\bar{1}11]$, $[1\bar{1}1]$, and $[11\bar{1}]$. For a field applied along [111] we would, therefore, expect two resonances, with

$$g_1=g_\parallel\ , \tag{14a}$$

and

$$g_2=(\tfrac{1}{9}g_\parallel^2+\tfrac{8}{9}g_\perp^2)^{1/2}. \tag{14b}$$

Misalignment would split the second of these into three lines, corresponding to slightly different angles between the field and the three local axes. A simple analysis shows that the average g value will still be given by Eq. (14b) above.

We now identify the three lines C, D, and E with g_2 and, taking the mean we find

$$g_\parallel^2+8g_\perp^2=179.6\ . \tag{15}$$

To identify the fourth line, we consider the two lines in group (iii) in the preceding section. Since we have no reason for picking one over the other we choose arbitrarily A_4 with $g_e=10.73$ but we note that A_2 would give a very similar result. This gives

$$g_\parallel^2=(10.73)^2=115.1\ , \tag{16}$$

and combining Eqs. (15) with Eq. (16), we find

$$\begin{aligned} g_\parallel&=10.73\ ,\\ g_\perp&=2.84\ . \end{aligned} \tag{17}$$

If we had chosen A_2 we would have deduced $g_\parallel=10.96$, $g_\perp=2.73$.

To check this analysis, we again turn to the results for $B\|[001]$. Our model predicts for this case one line with

$$g_3=(\tfrac{1}{3}g_\parallel^2+\tfrac{2}{3}g_\perp^2)^{1/2}=6.61,\ (6.71)\ , \tag{18}$$

where the value in parentheses corresponds to the second choice above. Misalignment will again split this line, this time into four components. If we examine Fig. 4 we see that we do indeed have a number of lines with g values in this general region. There are, in fact six lines but of these two (B and G) appear to be somewhat different in character (line shape and intensity) from the others. We, therefore, identify C, D, E, and F as the four resonances we expect. Taking the average g value we find $g_{\text{avg}}=6.70$ in excellent agreement with our prediction.

Using the g values given in Eq. (17) we can estimate the misalignment angles needed to explain the three lines for $B\|[111]$ and the four lines for $B\|[001]$. For the former we need $\delta\theta\sim 2°$, while for the latter $\delta\theta\sim 3°$, both within our limits of uncertainty.

These results provide strong evidence for Dy^{3+} on a sites in the crystal. Our analysis is not, however, without some difficulties. We have discussed all of the resonances only in terms of their g values, but not in terms of the corresponding internal field intercepts. The reason is simple: There is no unambiguous way to calculate such fields. If we were to assume that the internal fields are purely dipolar, we could calculate them using the g values and the lattice parameters, but this would ignore

the effects of nondipolar interactions, which are surely significant here. Even for nearest-neighbor c sites, nondipolar interactions account for more than one-third of the total coupling, and for the much shorter a-c bond we must expect considerably stronger interactions. Nor is it clear how one might parametrize such interactions. The symmetry is low and the basic mechanism is surely much more complex than simple Heisenberg exchange between the spins,[18] so that there is really no way to calculate the internal fields.

It must also be pointed out that our analysis has not explained a number of the observed resonances, so that there may well be some additional mechanisms which are important.

V. CONCLUSIONS

Our results may be summarized under two headings: those which were expected on the basis of previous understanding of DyAlG and those which were not. The former have confirmed the g value and the small Curie-Weiss θ, and the value of α_1 characterizing the strength of the nondipolar interactions between nearest neighbors. The agreement with previous estimates is in all cases very satisfactory.

The results which were in some sense unexpected were of two kinds. A number of lines were observed which can be ascribed to dimensional resonances arising from the fact that the wavelength of the radiation used was comparable to the sample size. The detailed analysis of such effects would be quite complicated under the conditions of the present experiments, and they were not studied further.

There were also a number of resonances which appear to be due to Dy^{3+} ions on a sites in the crystal lattice. There are some uncertainties in the detailed analysis, but the evidence is strong that in at least one melt-grown crystal, there is a measurable deviation from stoichiometry. Another melt-grown crystal containing 10% Dy and 90% Y did not show any additional lines.

Evidence for deviations from stoichiometry in melt-grown garnets has previously been found in various rare-earth gallium garnets.[19,20] A similar effect in rare-earth aluminum garnets is thus not surprising, and, indeed, there has been some indirect evidence in optical[21] and ultrasound absorption studies.[22] In the light of the present results, we have reexamined the lattice parameters measured by x rays for some of the crystals used in previous thermodynamic studies,[2] and Brandle[23] has also measured the lattice parameter for a piece from our current sample. In all cases the value of a_0 is slightly larger (by 0.0028–0.015 Å) than the smallest of the values determined for flux grown DyAlG, $a_0 = 12.038$ Å.[24] Brandle and Barns[20] have given an expression relating the difference between the lattice parameters Δa_0, and the parameter x characterizing the deviations from stoichiometry

$$x = 2\Delta a_0 / 1.615(r_{RE} - r_{Al}) , \tag{19}$$

where r_{RE} is the ionic radius of the rare earth ($Dy^{3+} = 0.908$ Å) and r_{Al} the radius of the ion it replaces ($Al^{3+} = 0.51$ Å). Substituting, we find values of x ranging from 0.009 to 0.046, with our present sample giving $x = 0.022$. Thus, on the basis of the x-ray data, we can estimate that about 0.7% of the a sites in our sample were occupied by Dy^{3+} ions. There are large uncertainties in these estimates, especially since the true stoichiometric value of a_0 is not known (another flux-grown sample gave a_0 $a_0 = 12.042$ Å),[25] but the order of magnitude for x is probably correct.

It is difficult to compare these estimates quantitatively with the results of our resonance measurements, since the transition probabilities enter the expressions for the intensities, and these are not known with any accuracy. Very roughly, we may estimate that the lines from the a sites will be a factor 100 more intense per spin than those for the c sites, since the g values perpendicular to the field are a factor of 10 larger and the intensity is proportional to $g_\perp^2$. Thus, it is not at all unreasonable that the intensities of the low-g-value lines should be very roughly comparable to that of the main line, as observed. A more detailed comparison would, of course, involve estimates of relative linewidths and also the fact that the low-g sites are not all equivalent, but for now we can conclude that the intensities of the observed spectra are quite consistent with the deviations from stoichiometry estimated from the x-ray data.

Our analysis indicates that the Dy^{3+} spins on the a sites are quite different from those on the c sites, with $g_\parallel \simeq 10.8$ and $g_\perp \simeq 2.8$, where the suffix $\parallel$ denotes one of the four $\{111\}$ directions. Their coupling to the c sites is generally quite complicated and we do not have enough information to describe it in detail. However, it is evident this coupling is quite strong, since the internal-field intercepts range from 0.3 to 1.1 T.

The effect of the a-site spins on the macroscopic properties of DyAlG can only be discussed qualitatively. We may note that the three pairs of c sites which are nearest neighbors to a particular a site will be parallel to one another in the usual antiferromagnetically ordered state of DyAlG, as they are in the present experiments. We can conclude, therefore, that the strong internal fields will also be effective in the antiferromagnetic state, so that the presence of the Dy^{3+} spins on the a sites will tend to stabilize the usual order. It does not seem unreasonable that a substitution of the order of 0.7% of the sites might cause changes in the ordering temperature by 1 or 2 %, as observed experimentally.

It is also tempting to speculate whether the presence of a-site spins might account for the puzzling neutron scattering which has been observed near the phase transition in applied magnetic fields along [110][5] and which has so far been explained only qualitatively in terms of a non-localized spin distribution.[6]

It seems clear that the detailed understanding of DyAlG would be simplified greatly if one could ensure that samples were accurately stoichiometric and free from other impurities. This may not be easy to achieve in practice. Crystals grown from the melt are intrinsically susceptible to small deviations from stoichiometry and crystals grown from a flux are susceptible to small inclusions or impurities. In both cases, great care is needed

to obtain essentially perfect crystals, and it is not clear that such crystals can indeed be grown in the case of DyAlG.

For now, the present experiments, together with the x-ray data, give an indication that existing samples do deviate from perfect stoichiometry, but that the deviation is not very large. For most analyses the deviation can therefore be neglected, but it must always be borne in mind whenever there are small inconsistencies in detailed comparisons of data obtained from different samples.

ACKNOWLEDGMENTS

We would like to thank K. Geeraert and B. Vrancken for assistance with the experiments and for many helpful discussions, and we are grateful to M. Ritter, C. P. Tigges, and I. Laursen for help with aligning the samples. We would also like to thank S. Geller and D. Brandle for valuable discussions concerning the possible deviations from stoichiometry, and D. Brandle and S. Mroczkowski for making the x-ray lattice parameter measurements. The crystal of $(Dy_{0.1}Y_{0.9})_3Al_5O_{12}$ was kindly grown for us by L. Rothrock. This work was supported in part by National Science Foundation Grant No. DMR 82-16222. One of us (W.P.W.) would also like to thank the Royal Society of London for financial support and the staff of the Clarendon Laboratory, Oxford, for their hospitality during the preparation of this paper.

APPENDIX: THIRD-ORDER ZEEMAN EFFECT

In low magnetic fields, the levels of a Kramers doublet split linearly with magnetic field but, as the field is increased, matrix elements to other levels will cause nonlinear effects. To third order

$$E_{\pm}=\pm\tfrac{1}{2}g\mu_B B+a_{\pm}B^2+b_{\pm}B^3 , \tag{A1}$$

where $\pm$ refer to the two components of the doublet. The splitting is thus

$$\Delta E=g\mu_B B+(a_+-a_-)B^2+(b_+-b_-)B^3+\cdots . \tag{A2}$$

We will now show that $a_+=a_-$ and $b_+=-b_-$ and estimate b_+ using perturbation theory.

Let us denote the ground-state doublet by $|\pm i\rangle$ and the excited doublets by $|\pm j\rangle$ at zero fields energies Δ_j. The corresponding first-order energy shifts in a field are $\pm\frac{1}{2}g_i\mu_B B$ and $\pm\frac{1}{2}g_j\mu_B B$. Using second-order perturbation theory, the energy of the lowest state $|-i\rangle$ is therefore

$$E_i=-\tfrac{1}{2}g_i\mu_B B-\sum_{\pm j}|P_{-i,\pm j}|^2/[\Delta_j+\tfrac{1}{2}\mu_B B(g_i\mp g_j)] , \tag{A3}$$

where the $P_{-i,\pm j}$ are the matrix elements of the magnetic moment operator. Assuming, as is usually the case, that $\Delta_j \gg \frac{1}{2}\mu_B B(g_i\mp g_j)$, we can expand the denominator and identify

$$a_-=-\sum_{\pm j}|P_{-i,\pm j}|^2/\Delta_j , \tag{A4}$$

$$b_-=\sum_{\pm j}\tfrac{1}{2}\mu_B(g_i\pm g_j)|P_{-i,\pm j}|^2/\Delta_j^2 . \tag{A5}$$

For the other component of the ground state, $|+i\rangle$, we find similarly

$$a_+=-\sum_{\pm j}|P_{+i,\pm j}|^2/\Delta_j , \tag{A6}$$

$$b_+=-\sum_{\pm j}\tfrac{1}{2}\mu_B(g_i\pm g_j)|P_{+i,\pm j}|^2/\Delta_j^2 . \tag{A7}$$

Using the fact that $|\pm i\rangle$ and $|\pm j\rangle$ are, respectively, time reversed conjugates, it follows that

$$|P_{-i,\pm j}|=|P_{+i,\mp j}| , \tag{A8}$$

so that

$$a_+=a_- \tag{A9}$$

and

$$b_+=-b_- . \tag{A10}$$

The ground-state splitting is thus

$$\Delta E=g_i\mu_B B+2b_+B^3$$

$$=g_i\mu_B B\left[1-\sum_{+j}\frac{(g_i\mp g_j)}{g_i\Delta^2}|P_{+i,\pm j}|^2B^2+\cdots\right] . \tag{A11}$$

The cubic correction coefficient, $2b_+$, can readily be estimated if the wave functions and energies of the low-lying states are known. In the case of DyAlG, a detailed crystal-field analysis has been carried out by Lewis[26] and, summing over the states belonging to the $J=\frac{15}{2}$ term, we find for $B\|0z$

$$\Delta E=17.8\mu_B B(1-0.98\times10^{-4}B^2) , \tag{A12}$$

where B is measured in tesla. In evaluating the different contributions, care must generally be taken to assign the correct *signs* to the various g_j relative to g_i. In the present case $|g_i|>|g_j|$ for all the excited states, so that $(g_i\mp g_j)/g_i>0$ and the terms in the correction are, therefore, negative. For other cases and, indeed, for other orientations of the field, both signs are possible.

The ground-state g value predicted by Lewis' wave functions is in good agreement with the experimental value (Sec. IV) and this, together with the agreement for g value and energies for other levels,[26] suggests that our value for b_+ should be reasonably accurate. It is hard to estimate the uncertainty, since there are many contributions. However, we may note that the major contribution to b_+ (85%) comes from the first excited doublet, whose energy is predicted as 63.6 cm^{-1}, compared to the experimental value[10] of 69.0 cm^{-1}, which would make our estimate for b_+ too high by some 17%. The uncertainty in the corresponding matrix element cannot readily be es-

timated, but it could be quite small since the major contribution comes from only one term (the $J_z = +\frac{15}{2}$ components), which should be relatively well determined.

We estimate, therefore, somewhat subjectively, our final value for the correction due to the third-order Zeeman effect as

$$\Delta E = g\mu_B B[1-(0.8\pm0.3)\times10^{-4}B^2] , \quad (2')$$

which is the expression used in Sec. IV A.

[1]W. P. Wolf, D. P. Landau, B. E. Keen, and B. Schneider, Phys. Rev. B **5**, 4472 (1972).

[2]D. P. Landau, B. E. Keen, B. Schneider, and W. P. Wolf, Phys. Rev. B **3**, 2310 (1971).

[3]F. Bertaut and F. Forrat, C. R. Acad. Sci. (Paris) **243**, 1219 (1956).

[4]R. Faulhaber and S. Hüfner, Solid State Commun. **7**, 389 (1969).

[5]M. Blume, L. M. Corliss, J. M. Hastings, and E. Schiller, Phys. Rev. Lett. **32**, 544 (1974).

[6]D. Mukamel and M. Blume, Phys. Rev. B **15**, 4516 (1977).

[7]R. W. Sanders, R. M. Belanger, M. Motokawa, V. Jaccarino, and S. M. Rezende, Phys. Rev. B **23**, 1190 (1981).

[8]P. Janssen, Solid State Commun. **50**, 655 (1984).

[9]B. E. Argyle, J. L. Lewis, R. L. Wadsack, and R. K. Chang, Phys. Rev. B **4**, 3035 (1971), and references cited therein.

[10]See, for example, Ref. 1 and references cited therein.

[11]P. Janssen, I. De Wolf, and I. Laursen, J. Phys. Chem. Solids **46**, 1387 (1985).

[12]D. J. E. Knight, National Physical Laboratory, Report No. QU45, 1981.

[13]D. P. Landau and B. E. Keen, Phys. Rev. B **10**, 4805 (1979).

[14]M. Steiner and N. Giordano, Phys. Rev. B **25**, 6886 (1982), and references cited therein.

[15]B. Schneider, D. P. Landau, B. E. Keen, and W. P. Wolf, Phys. Lett. **23**, 210 (1966).

[16]B. E. Keen, D. P. Landau, and W. P. Wolf, Phys. Lett. **23**, 202 (1966).

[17]W. P. Wolf, M. Ball, M. T. Hutchings, M. J. M. Leask, and A. F. G. Wyatt, J. Phys. Soc. Jpn. **17**, Suppl. **B1**, 443 (1962).

[18]W. P. Wolf, J. Phys. (Paris) Colloq. **32**, C1-26 (1971).

[19]S. Geller, Z. Kristallogr. **125**, 1 (1967).

[20]C. D. Brandle and R. L. Barnes, J. Cryst. Growth **26**, 169 (1974).

[21]Yu. K. Voron'ko and A. A. Sobol', Phys. Status Solidi A **27**, 257 (1975); A **27**, 657 (1975).

[22]S. N. Ivanov, V. V. Medved', and A. N. Makletsov, Fiz. Tverd. Tela (Leningrad) **26**, 1832 (1984) [Sov. Phys.—Solid State **26**, 1108 (1984)].

[23]C. D. Brandle (private communication).

[24]K. L. Keester and G. G. Johnson, Jr., J. Appl. Crystallogr. **4**, 178 (1971).

[25]C. B. Rubinstein and R. L. Barnes, Amer. Mineral. **49**, 1489 (1964).

[26]J. L. Lewis, Ph.D. thesis, Yale University, 1971.